

# The Structure and Possible Catalytic Sites of Mo<sub>3</sub>S<sub>9</sub> as a Model of Amorphous Molybdenum Trisulfide: A Computational Study

Haijun Jiao,<sup>\*,†,‡</sup> Yong-Wang Li,<sup>§</sup> B. Delmon,<sup>||</sup> and Jean-François Halet<sup>‡</sup>

Contribution from the Laboratoire de Chimie du Solide et Inorganique Moléculaire, UMR 6511 CNRS, Université de Rennes 1, Institut de Chimie de Rennes, F-35042 Rennes Cedex, France, Institut für Organische Chemie, Universität Erlangen-Nürnberg, Henkestrasse 42, D-91054 Erlangen, Germany, State Key Laboratory of Coal Conversion, Institute of Coal Chemistry, Chinese Academy of Sciences, 030001, Taiyuan, China, and Unité de Catalyse et Chimie des Matériaux Divisés, Université Catholique de Louvain, Louvain-la-Neuve, B-1348, Belgium

Received September 18, 2000. Revised Manuscript Received May 7, 2001

**Abstract:** The structure and reactivity of Mo<sub>3</sub>S<sub>9</sub> clusters, taken as a model for amorphous molybdenum trisulfide, have been investigated at the B3LYP density functional level of theory. Two computed ground-state cluster structures are close in energy and have similar structural parameters and vibrational modes. These values agree well with the available experimental data. These cluster structures are considered to be formed simultaneously during the preparation process of catalysts. Their catalytic activity has been analyzed on the basis of frontier molecular orbital properties (FMO). It is mainly due to 4d-type orbitals of the unsaturated molybdenum centers without terminal sulfur coordination. The small HOMO–LUMO gaps suggest that Mo<sub>3</sub>S<sub>9</sub> clusters can act as Lewis acids or Lewis bases.

## Introduction

Molybdenum sulfides (MoS<sub>x</sub>) are widely used as catalysts in oil refineries for hydrogenation (HYD), hydrodesulfurization (HDS), and hydrodenitrogenation (HDN) reactions, which currently receive special attention for producing cleaner fuels.<sup>1</sup> It is widely agreed that one of the main active components for these hydrotreating processes on a stable catalyst surface is molybdenum disulfide MoS<sub>2</sub> with a S–Mo–S-layered sandwich structure, on which the edge sites play crucial roles in the catalytic reactions.<sup>1</sup> However, detailed structural information concerning the properties of such structures is still unclear. The recent experimental discovery of supported triangular nanostructures of MoS<sub>2</sub> by using high-resolution scanning tunneling microscopy (HRSTM) renewed the interest in the variability of the important catalyst that MoS<sub>2</sub> represents.<sup>2</sup>

Initially, just after sulfidation of MoO<sub>3</sub>, molybdenum sulfide catalysts are found to be amorphous at the start,<sup>3–5</sup> and high-resolution electron microscopy (HREM) consistently shows a highly disordered “rag” structure. The structure of this amor-

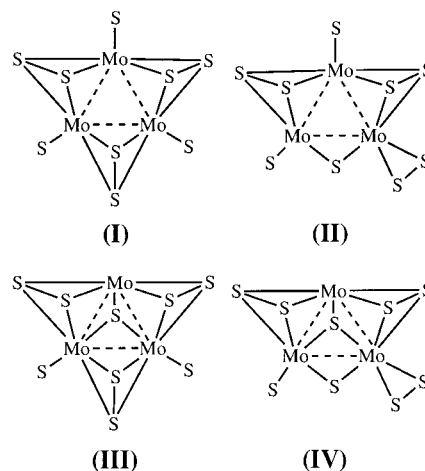


Figure 1. Four proposed Mo<sub>3</sub>S<sub>9</sub> structures.

phous form of molybdenum sulfide was investigated by using X-ray absorption spectroscopy.<sup>3</sup> The extended X-ray absorption fine structure (EXAFS) data revealed two Mo–Mo separations of 274.5 ± 6.6 and 315.8 ± 7.1 pm, and an average Mo–S bond length of 244 ± 9 pm. On the basis of monochromatic X-ray photoemission (XPS) and vibrational spectroscopy, Weber et al.<sup>4</sup> found that the intermediate of the MoS<sub>2</sub> active phase in HDS catalysts is amorphous MoS<sub>3</sub> which should be essentially an aggregation of Mo<sub>3</sub>S<sub>9</sub> cluster units, and that all the molybdenum centers in the intermediate have the characteristic Mo(IV) formal oxidation state and at least two types of sulfur ligands (S<sup>2-</sup> and S<sub>2</sub><sup>2-</sup>) in different coordination spheres. Several possible microstructures, I–IV, were proposed (Figure 1).<sup>4</sup>

(5) (a) Müller, A.; Diemann, E.; Branding, A.; Baumann, F. W.; Breyse, M.; Vrinat, M. *Appl. Catal.* **1990**, *62*, 113. (b) Brito, J. L.; Severino, F.; Delgado, N. N.; Laine, J. *Appl. Catal. A* **1998**, *173*, 193. (c) Diemann, E.; Weber, T.; Müller, A. *J. Catalysis* **1994**, *148*, 288 and references therein.

<sup>†</sup> Université de Rennes 1.

<sup>‡</sup> Universität Erlangen-Nürnberg.

<sup>§</sup> Chinese Academy of Sciences.

<sup>||</sup> Université Catholique de Louvain.

(1) (a) Delmon, B. In *Catalysts in Petroleum Refining-1989*; Trimm, D. L., Akashah, S., Absi-Halabi, M., Bishara A., Eds.; Elsevier: Amsterdam, 1990; pp 1–40. (b) Delmon, B.; Froment, G. *Catal. Rev. Sci. Eng.* **1996**, *38*, 69. (c) Topsøe, H.; Clausen, B. S.; Franklin, F. E.; Massoth, E. In *Science and Technology in Catalysis: Hydrotreating Catalysis*; Abderson, J. R., Boudart, M., Eds.; Springer, Berlin, 1996; Vol. 11. (d) Startsev, A. N. *Catal. Rev. Sci. Eng.* **1995**, *37*, 353. (e) Startsev, A. N. *J. Mol. Catal.* **2000**, *152*, 1.

(2) Helveg, S.; Lauritsen, J. V.; Lae Gsgaard, E.; Stensgaard, I.; Nørskov, J. K.; Clausen, B. S.; Topsøe, H.; Besenbacher, F. *Phys. Rev. Lett.* **2000**, *84*, 951.

(3) Cramer, S. P.; Liang, K. S.; Jacobson, A. J.; Chang, C. H.; Chianelli, R. R. *Inorg. Chem.* **1984**, *23*, 1215.

(4) Weber, T.; Muijsers, J. C.; Niemantsverdriet, J. W. *J. Phys. Chem.* **1995**, *99*, 9194.

However, the origin of the catalytic activity of the amorphous structures during the HDS process is not well understood. Diemann et al.<sup>5c</sup> also pointed out that the noncrystalline character of the catalyst hinders an accurate X-ray structure determination, and the existence of many adjustable parameters during the preparation of the catalyst and during the course of the reaction itself is the main reason why many of the reported results are not really comparable.

High-level density functional theory (DFT) computations were carried out on the proposed Mo<sub>3</sub>S<sub>9</sub> clusters (**I–IV**, Figure 1) based on the EXAFS structural information.<sup>3,4</sup> These “molecular” structures were chosen to reasonably mimic the properties of amorphous MoS<sub>3</sub>, in particular of maintaining the formal Mo(IV) oxidation state in the clusters as proposed by Weber et al. from XPS spectra.<sup>4</sup> The goals of these investigations were: (a) to compare the computed structural parameters and vibrational frequencies for the amorphous MoS<sub>3</sub> with the available experimental data to get deeper insights into the structural features of the MoS<sub>3</sub> phase, and (b) to explore the reasons of the catalytic activity of the amorphous MoS<sub>3</sub> phase for hydrotreating reactions over MoS<sub>2</sub> type catalysts, on the basis of the frontier molecular orbital (FMO) features.

Despite the reasonable agreement between the computed and available experimental data, it is necessary to point out that the employed molecular systems for modeling the complicated real catalysts are very approximated and limited, and the FMO analysis of the catalytic activity is only qualitative. For example, the degree and thermodynamic properties of cluster aggregations, being very sensitive to the catalytic activity, were not taken into account, and this can only be understood well via systematic studies of the interaction between catalyst and reactants. The role of support was also not considered. Therefore, detailed investigation into this useful and interesting industrial process should be the ongoing experimental and theoretical work.

### Computational Details

Geometry optimizations were carried out at the B3LYP density functional level of theory<sup>6</sup> with the LANL2DZ basis set including a set of polarization functions (LANL2DZp).<sup>7</sup> All optimized structures were characterized by frequency calculations at the same level of theory. With the calculated number of imaginary frequencies ( $N_{\text{Imag}}$ ), the optimized structures were characterized to be energy minima ( $N_{\text{Imag}} = 0$ ), transition states ( $N_{\text{Imag}} = 1$ ), or higher-order saddle points ( $N_{\text{Imag}} > 1$ ) on the potential energy surfaces (PES). All of the calculations were performed with the Gaussian98 program.<sup>8</sup> The computed energetic data are given in Table 1.

### Results

Figure 2 shows the (**I–IV**) optimized Mo<sub>3</sub>S<sub>9</sub> cluster structures on the basis of those proposed by Weber et al.<sup>4</sup> Structure **I** has  $D_{3h}$  symmetry, and the three molybdenum atoms are in a triangular arrangement. Each molybdenum center is connected to five sulfur atoms, that is, two  $-S_2-$  bridges and one  $-S$  terminal coordination. The Mo–Mo separation is 361.8 pm, and the terminal Mo–S bond length of 210.7 pm is largely shorter than those between molybdenum and bridging sulfurs (249.3

**Table 1.** B3LYP/LANL2DZp Zero-Point Energies (ZPE, kJ/mol), Number of Imaginary Frequencies ( $N_{\text{Imag}}$ ), Total Electronic Energies ( $E_{\text{tot}}$ , au) and the Relative Energies ( $E_{\text{rel}}$ , kJ/mol)

	ZPE <sup>a</sup> ( $N_{\text{Imag}}$ )	$E_{\text{tot}}$	$E_{\text{rel}}$ <sup>b</sup>
<b>I</b>	40.2 (3)	−293.95613	102.9
<b>II</b>	39.7 (4)	−293.84719	388.3
<b>III</b>	44.8 (0)	−293.98754	25.0
<b>IV</b>	44.4 (0)	−293.99689	0.0

<sup>a</sup> ZPE, scaled by 0.97. <sup>b</sup> At B3LYP/LANL2DZp + ZPE.

pm). The S–S distance in the  $-S_2-$  bridge is 212.4 pm. However, the optimized structure (**I**) has three imaginary frequencies and therefore corresponds to a higher-order saddle point rather than an energy minimum on the PES.

The  $C_s$  symmetrical structure **II** can be derived from structure **I** by exchanging the positions of the S8–S9 bridge and the S3 terminal atom (Figure 2). The computed Mo–Mo separations are in the range of 300.0–347.7 pm, and the S–S distance of the terminal  $-S_2$  (199.6 pm) is shorter than those of the bridging  $-S_2-$  (205.8–212.3 pm). The terminal Mo–S distances are shorter than those between molybdenum and the bridging or terminal S<sub>2</sub> units. However, structure **II** has four imaginary frequencies ( $N_{\text{Imag}} = 4$ ) and also corresponds to a higher-order saddle point on the PES.

In contrast to **I** and **II**, the proposed structures **III** and **IV** are found to be true energy minima on the PES according to the frequency calculations ( $N_{\text{Imag}} = 0$ ). Structure **III** has  $C_s$  symmetry, whereas **IV** is  $C_1$ -symmetrical. At the B3LYP/LANL2DZp level, **IV** is the most stable isomer, and **III** is only 25.0 kJ/mol higher in energy, while **I** and **II** are much higher in energy (Table 1). Thus, our computations show that only two Mo<sub>3</sub>S<sub>9</sub> structural isomers proposed by Weber et al.<sup>4</sup> might be really formed and participate in the catalytic process.

It should be noted that the optimized structures **III** and **IV** differ somewhat from those proposed by Weber et al.<sup>4</sup> The structure proposed for **III** has three  $-S_2-$  bridging units, and each of them spans one Mo–Mo bond. However, the computed structure shows one  $-S_2-$  and two  $-S-$  edge-bridging units and two  $-S$  terminal units, as well as one S atom and one S<sub>2</sub> face-bridging units (Figure 2). A similar situation is also found for structure **IV**.

In **III**, there are two Mo–Mo separations of 276.1 and 317.8 pm, and the terminal Mo–S distance of 214.7 pm is shorter than those of the bridges, which are in the range of 241.2–261.4 pm. The edge-bridging unit has a S–S distance of 207.3 pm, and the apical capping sulfur (S1) has the Mo–S distances of 233.1 and 252.0 pm. The Mo–S distances of the face-bridging S<sub>2</sub> unit are 241.5 and 254.1 pm, and the S–S bond length is 226.7 pm.

Structure **IV** has a shape somewhat similar to **III** and can be derived from structure **III** by exchanging the position of the terminal S7 and the bridging S8–S9. Compared to **III**, there are two shorter Mo–Mo distances of 282.3 and 277.9 pm, and a longer one of 359.2 pm. The Mo–S lengths are close to those

(6) (a) Becke, A. D. *J. Chem. Phys.* **1993**, *98*, 5648. (b) Foresman, J. B.; Frisch, A. *Exploring Chemistry with Electronic Structure Methods: A Guide to Using Gaussian*, 2nd ed.; Gaussian, Inc.: Pittsburgh, PA, 1996.

(7) For LANL2DZp basis set: (a) Hay, P. J.; Wadt, W. R. *J. Chem. Phys.* **1985**, *82*, 299. (b) Dunning, T. H., Jr.; Hay, P. J. In *Modern Theoretical Chemistry*; Schaefer, H. F., III, Ed.; Plenum Press: New York, 1976; pp 1–28. (c) For polarization functions see: Huzinaga, S.; Anzelm, J.; Klobukowski, M.; Radzio-Andzelm, E.; Sakai, Y.; Tatewaki, H. *Gaussian Basis Sets for Molecular Calculations*, Elsevier: Amsterdam, 1984.

(8) Frisch, M. J.; Trucks, G. W.; Schlegel, H. B.; Scuseria, G. E.; Robb, M. A.; Cheeseman, J. R.; Zakrzewski, V. G.; Montgomery, J. A., Jr.; Stratmann, R. E.; Burant, J. C.; Dapprich, S.; Millam, J. M.; Daniels, A. D.; Kudin, K. N.; Strain, M. C.; Farkas, O.; Tomasi, J.; Barone, V.; Cossi, M.; Cammi, R.; Mennucci, B.; Pomelli, C.; Adamo, C.; Clifford, S.; Ochterski, J.; Petersson, G. A.; Ayala, P. Y.; Cui, Q.; Morokuma, K.; Malick, D. K.; Rabuck, A. D.; Raghavachari, K.; Foresman, J. B.; Cioslowski, J.; Ortiz, J. V.; Stefanov, B. B.; Liu, G.; Liashenko, A.; Piskorz, P.; Komaromi, I.; Gomperts, R.; Martin, R. L.; Fox, D. J.; Keith, T.; Al-Laham, M. A.; Peng, C. Y.; Nanayakkara, A.; Gonzalez, C.; Challacombe, M.; Gill, P. M. W.; Johnson, B. G.; Chen, W.; Wong, M. W.; Andres, J. L.; Head-Gordon, M.; Replogle, E. S.; Pople, J. A. *Gaussian 98*, revision A.5; Gaussian, Inc.: Pittsburgh, PA, 1998.

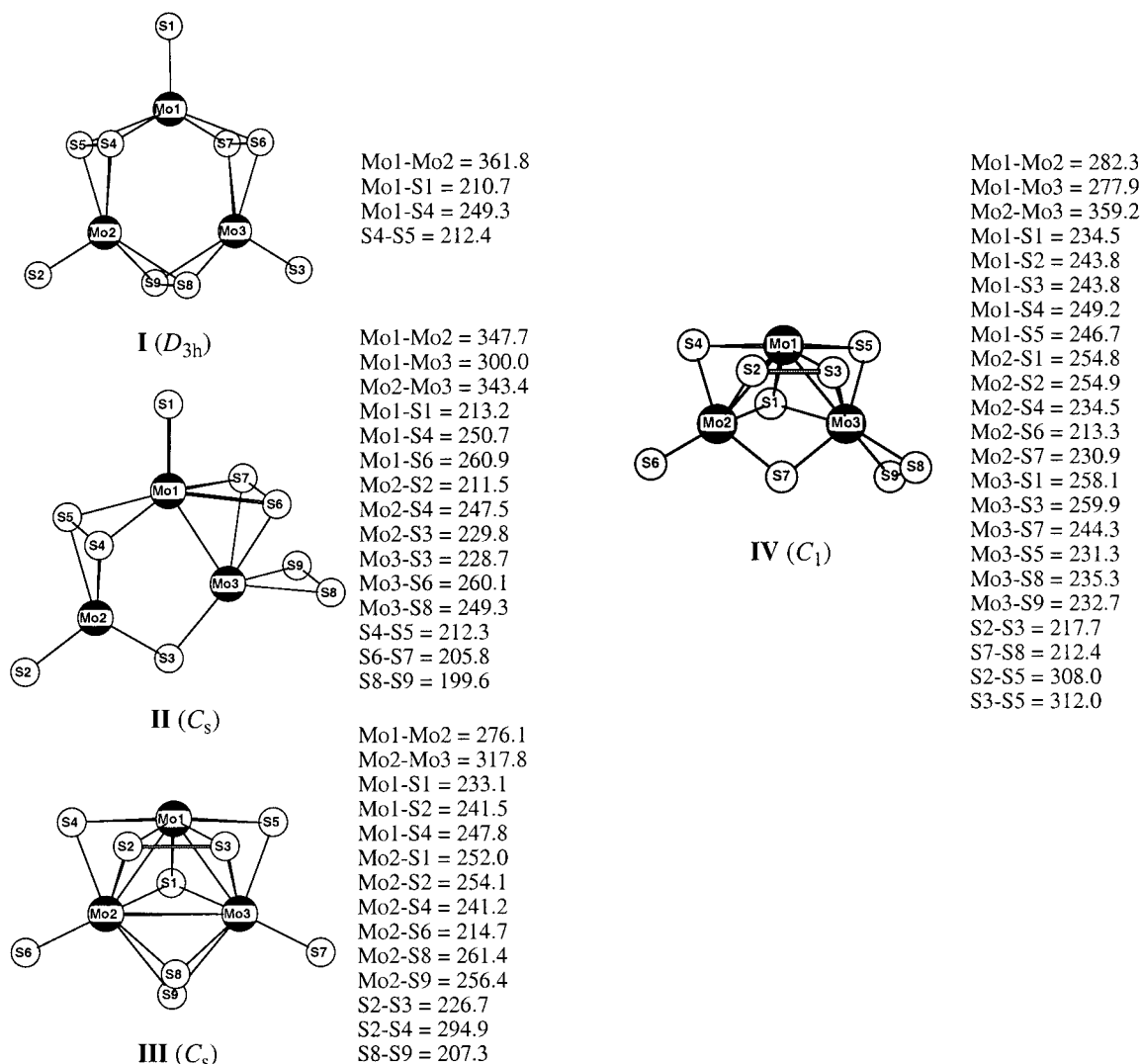


**Figure 2.** B3LYP/LANL2DZp distances (pm) for I–IV.

computed in structure **III**. On the basis of the structural similarity and small energy difference between **III** and **IV** (25 kJ/mol), extensive calculations for locating the corresponding transition state were carried out but without success due to convergence problems.

## Discussion

A comparison between the computed structural results for  $\text{Mo}_3\text{S}_9$  clusters and the available EXAFS data is useful and informative. Cramer et al.<sup>3</sup> found two significantly distinct Mo–Mo distances of 274.6 and 315.8 pm and an average Mo–S distance of 244 pm for the amorphous form. These findings are very close to those of the optimized structure **III**, in which the calculated Mo–Mo distances are 276.1 and 317.8 pm (Figure 2). This constitutes a very nice agreement between theory and experiment. It is also worth mentioning that the recent EXAFS measurement by de Bont et al.<sup>9a</sup> showed that there are two distinguishable Mo–Mo separations (278 and 316 pm) in the catalytically active molybdenum sulfide particles formed inside the supercages of NaY zeolite used as a hydrotreating

catalyst. According to our calculations (Figure 2), the terminal Mo–S distance (214.7 pm) is significantly shorter than the bridging values (233.1–256.9 pm), but the average values are close to the EXAFS data<sup>3</sup> (it is not possible to obtain an unequivocal determination of multiple Mo–S distances in experiments). Computed structural parameters for structure **IV** with the close Mo–Mo distances of 277.9 and 282.3 pm are also in the range of the experimental values.<sup>3</sup>

Weber et al. reported the infrared spectrum of the  $\text{MoS}_3$  phase.<sup>4</sup> Since the spectra for the amorphous molybdenum trisulfide showed very broad and badly resolved bands, the assignment of the vibrational modes was deduced from the spectrum of the well-structured  $(\text{NH}_4)_2[\text{Mo}_3\text{S}_{13}] \cdot \text{H}_2\text{O}$  cluster.<sup>4</sup> The bands at 545, 520, and 470  $\text{cm}^{-1}$  were considered to correspond to the S–S stretching frequencies of the bridging ( $-\text{S}_2-$ ) and terminal  $-\text{S}_2$  units and that of the molybdenum triply capping sulfur bonds, respectively. Other lower values were ascribed to combined modes.<sup>4</sup>

The B3LYP/LANL2DZp vibrational frequencies with their possible displacement vectors for **III** and **IV** are shown in Figures 3 and 4, respectively. For **III**, the largest vibrational mode at 534  $\text{cm}^{-1}$  is the S–S stretching band of the bridging  $-\text{S}_2-$  unit (S8–S9), and the next modes are the symmetrical (519  $\text{cm}^{-1}$ ) and asymmetrical (511  $\text{cm}^{-1}$ ) stretching frequencies

(9) (a) de Bont, P. W.; Vissenberg, M. J.; de Beer, V. H. J.; van Veen, J. A. R.; van Santen, R. A.; van der Kraan, A. M. *Appl. Catal. A* **2000**, *202*, 99. (b) Cattaneo, R.; Weber, Th.; Shido, T.; Prins, R. *J. Catal.* **2000**, *191*, 225. (c) Leliveld, R. G.; van Dillen, A. J.; Geus, J. W.; Koningsberger, D. C. *J. Catal.* **1997**, *171*, 115.

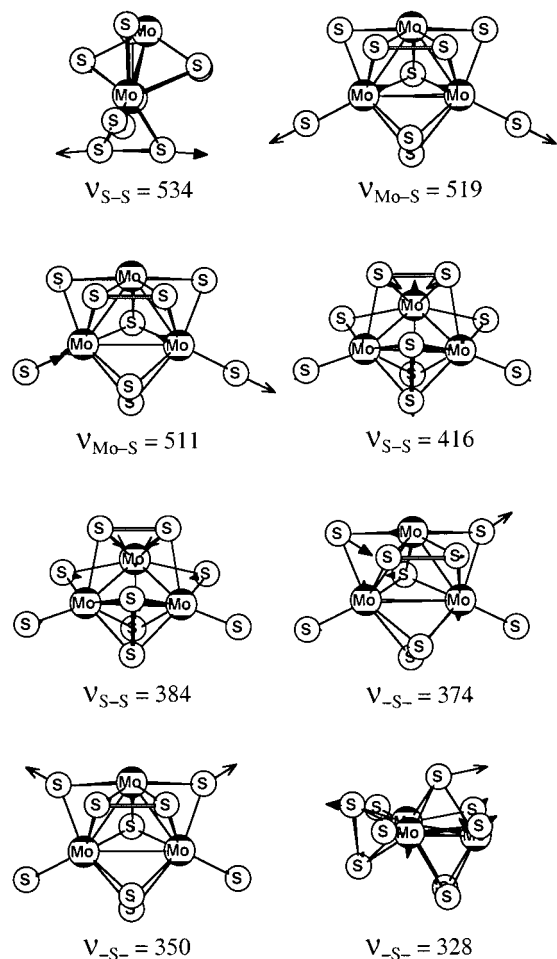


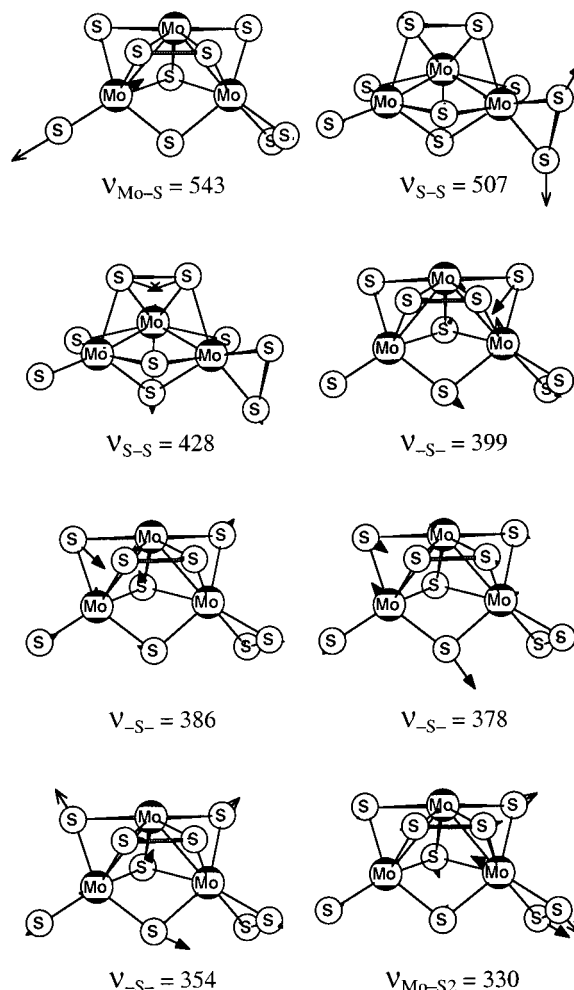
**Figure 3.** B3LYP/LANL2DZp computed vibrational frequencies ( $\nu$ ,  $\text{cm}^{-1}$ ) for **III** (the arrows show the vibrational modes).

of the terminal Mo–S bond (Figure 3). For **IV**, the largest vibrational mode at  $543 \text{ cm}^{-1}$  is the terminal Mo–S stretching, and the next one at  $507 \text{ cm}^{-1}$  is that of the terminal  $-\text{S}_2$  bridge (Figure 4).

By combining the features of **III** and **IV**, we can reproduce most of the bands of the experimental spectrum obtained by Weber et al.<sup>4</sup> However, the proposed Mo–S (triply bridging) stretching at  $470 \text{ cm}^{-1}$  cannot be reproduced, and the corresponding computed modes have lower values and intensities for both the  $-\text{S}$  and  $-\text{S}_2-$  capping units. It might be due to the possible mixture of both structures with an undefined distribution ratio of masses, and their overlap or combined spectra made an unequivocal assignment of some experimental frequencies impossible. Moreover, this situation can also be further complicated by random packing aggregation, or by other unknown structural isomers or related structures. An experimental reinvestigation of the MoS<sub>3</sub> structures would be helpful.<sup>10</sup>

At this stage, it is impossible to decide on the existence of one structure of Mo<sub>3</sub>S<sub>9</sub> cluster and to exclude the other one. The small energy difference between **III** and **IV** (25 kJ/mol), their close structural parameters, and also their very similar vibrational modes might suggest that they form simultaneously during the preparation of molybdenum sulfide catalysts and can easily transform to each other. Therefore, their random packing may correctly describe the MoS<sub>3</sub> amorphous phase with loose connections between cluster units via S bridges in the bulk of the material.

Assuming that the intermediate structures of MoS<sub>2</sub> catalysts for HDS<sup>1,5,9</sup> and Fischer–Tropsch<sup>11</sup> reactions at the initial stages

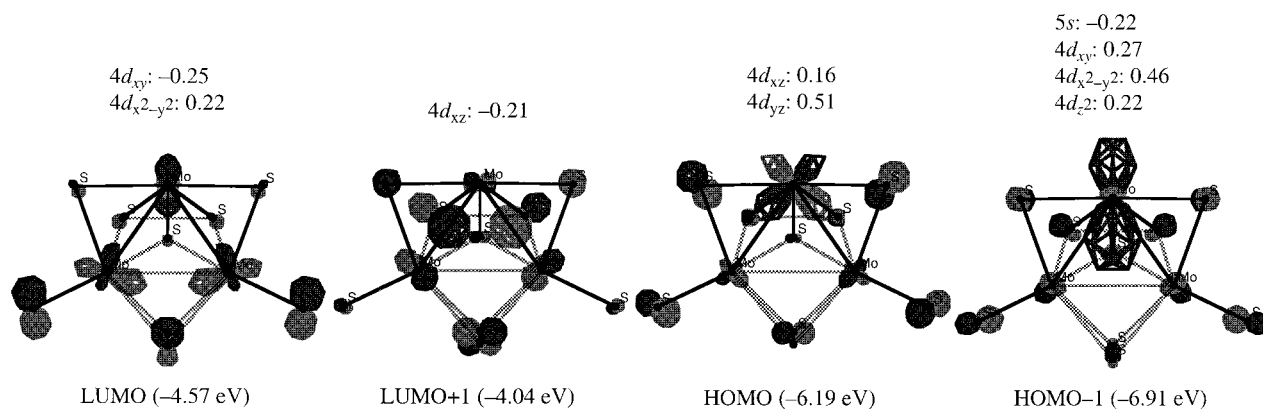
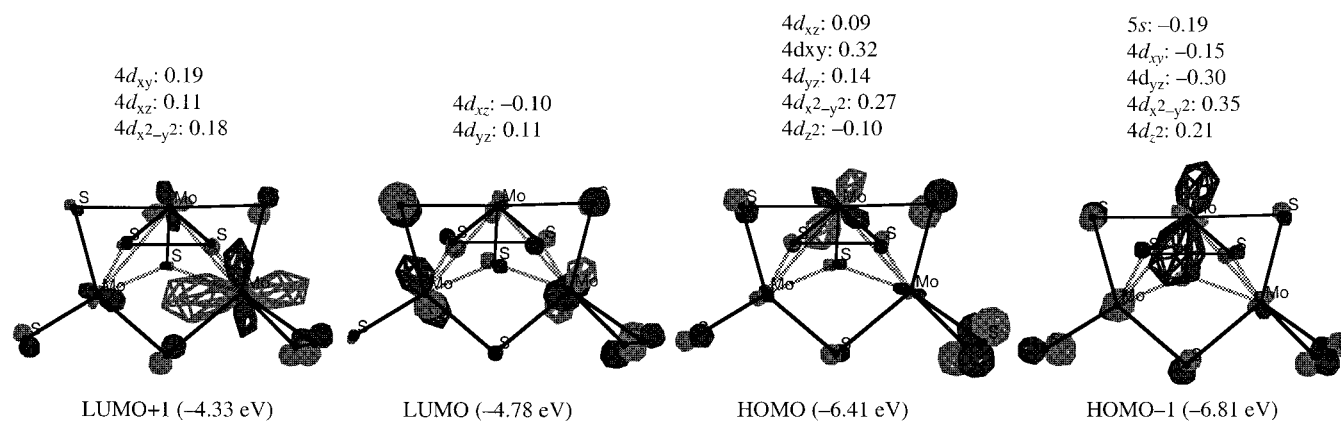


**Figure 4.** B3LYP/LANL2DZp computed vibrational frequencies ( $\nu$ ,  $\text{cm}^{-1}$ ) for **IV** (the arrows show the vibrational modes).

after their preparation consist mainly of MoS<sub>3</sub>-type phases containing catalytically active Mo<sub>3</sub>S<sub>9</sub> cluster units, it is informative to look at the composition of the orbitals located at the HOMO–LUMO region for the computed clusters. Consequently, the frontier molecular orbitals (FMO) of the Mo<sub>3</sub>S<sub>9</sub> units **III** and **IV** were analyzed on the basis of DFT calculations. Figures 5 and 6 show the HOMO/HOMO – 1 and LUMO/LUMO + 1 of **III** and **IV** with their energies and the atomic orbital coefficients in the FMOs of the unsaturated molybdenum

(10) Due to the possible aggregation of the Mo<sub>3</sub>S<sub>9</sub> cluster units in the experiment, one of the reviewers pointed out that the occurrence of covalent bonds between the clusters was not taken into account by the theoretical Mo<sub>3</sub>S<sub>9</sub> models used since the “broken bonds” were not saturated. However, calculations carried out on “saturated models” show that saturation of the broken bonds with hydrogen, for example, leads to the loss of the characteristic Mo–Mo distances and vibrational frequencies which are the essential central points of the extensive experimental work reported in refs 3 and 4. This is mainly due to the fact that any saturation at the terminal sulfur atoms will change the formal oxidation state from Mo(IV) into Mo(III), in disagreement with the XPS findings given in ref 4. It turns out that only the Mo<sub>3</sub>S<sub>9</sub> models used in this work have the characteristic bond distances, vibrational data, and the formal Mo(IV) oxidation state as found in experiments and should be representative for amorphous MoS<sub>3</sub>. Therefore, the saturated models are not appropriate for studying the MoS<sub>3</sub> catalyst freshly prepared at high temperature, and experimental reinvestigation of this catalytic active species is very much desired. For further discussions of the amorphous molybdenum trisulfide structures, see: Hibble, S. J.; Walton, R. I.; Pickup, D. M.; Hannon, A. C. *J. Non-Cryst. Solids* **1998**, 232–234, 434 and Walton, R. I.; Dent, A. J.; Hibble, S. J. *Chem. Mater.* **1998**, 10, 3737.

(11) Close, M. R.; Petersen, J. L.; Kugler, E. L. *Inorg. Chem.* **1999**, 38, 1535 and references therein.

Figure 5. Frontier molecule orbitals for **III**.Figure 6. Frontier molecule orbitals for **IV**.

centers (without terminal sulfur), which is thought to be responsible for the catalytic activity. The unsaturated Mo centers in **III** and **IV** contribute significantly to the occupied and the virtual orbitals, mainly through 4d-type orbital participation. A similar phenomenon was found for the Mo corner sites in MoS<sub>2</sub> structures in a study based on SCF-MO calculations.<sup>12</sup>

It should be noted that the energy differences between HOMO and LUMO are only 2.15 eV for **III** and 2.08 eV for **IV**. This indicates that both electron-accepting and electron-donating properties (Lewis acid and Lewis base features) of the unsaturated Mo sites can be essential for the activation of reactants, for example, in HDS and potentially for CO activation in Fischer–Tropsch reactions.<sup>12–14</sup> These dual properties explain their strong attachment to acidic supports and the adsorption affinity for unsaturated functions in catalytic reactions. In addition, orbitals which are only slightly lower than HOMO (HOMO - 1) or higher than LUMO (LUMO + 1) may also be important when considering the electron-donating and electron-accepting properties of the unsaturated Mo sites (Figures 5 and 6).

Although the possible adsorption of reactant molecules on the active Mo site is not considered here, the results strongly suggest that the unsaturated Mo centers in the Mo<sub>3</sub>S<sub>9</sub> clusters may possess a unique catalytic activity for chemical reactions in hydrotreating and Fischer–Tropsch processes. Deposited on alumina<sup>5a</sup> or carbon,<sup>5b</sup> (NH<sub>4</sub>)<sub>2</sub>[Mo<sub>3</sub>S<sub>13</sub>]·H<sub>2</sub>O clusters likely lose

NH<sub>3</sub> and H<sub>2</sub>O in the reaction conditions, and they were found to be very active in hydrotreating reactions. In relation with the thiophene HDS studies suggesting a significant activity of MoS<sub>x</sub> catalysts,<sup>5</sup> the higher initial activity of catalysts has not been clearly attributed to the MoS<sub>3</sub> phase, although it had been claimed that the freshly sulfided phase of molybdenum is likely to be of the MoS<sub>3</sub> type.<sup>3–5,9</sup> There are strong arguments for concluding that the stable catalytic phase in HDS catalysis is MoS<sub>2</sub>. However, analyses very often indicate a sulfur excess over stoichiometry.<sup>11</sup> Moreover, high-resolution transmission electron microscopy (HRTEM) on catalysts, having worked for some time, shows structures that do not correspond to MoS<sub>2</sub>.<sup>9a</sup> MoS<sub>3</sub>-like structures containing Mo<sub>3</sub>S<sub>9</sub> cluster units may actually contribute to the overall activity.

Directly related to the present study are recent investigations on the catalytic reactivity of molybdenum sulfide particles deposited inside the supercages of NaY zeolite.<sup>9a</sup> In this case, the constraints imposed by the limited size of the cavities hinder the formation of large aggregates and permit the maintenance of the dispersion of the small molybdenum sulfide species inside the zeolite supercages. This may explain the higher HDS catalytic activity at the initial stage of the freshly prepared catalysts.<sup>9a</sup>

## Conclusions

To our knowledge this is the first time the structure and the potential catalytic activity of amorphous MoS<sub>3</sub> which may contain Mo<sub>3</sub>S<sub>9</sub> cluster units have been investigated using the high-level B3LYP density functional theory. Two of the cluster structures proposed by Weber et al. are found to be true ground states (energy minima), which differ only slightly in energy (by 25 kJ/mol). The optimized structural parameters and the

(12) Li, Y.-W.; Pang, X.-Y.; Delmon, B. *J. Phys. Chem. A* **2000**, *104*, 11375.

(13) Raybaud, P.; Hafner, H.; Kresse, G.; Toulhoat, H. *Phys. Rev. Lett.* **1998**, *80*, 1481.

(14) Fohlisch, A.; Nyberg, M.; Bennich, P.; Triguero, L.; Hasselstrom, J.; Karis, O.; Pettersson, L. G. M.; Nilsson, A. *J. Chem. Phys.* **2000**, *112*, 1946.

computed vibrational frequencies are close to each other. They agree well with the available EXAFS results and can be related to available infrared spectra. Our findings suggest that both structures might be formed and perhaps transform to each other during the preparation of the catalysts or during the course of the reaction.

On the basis of the frontier molecular orbitals, the active centers of the catalytic reactions are presumably on the unsaturated molybdenum centers (without terminal sulfur coordination) in the structures shown to be likely present in catalysts. They strongly contribute to the FMO mainly through

4d-type atomic orbitals. The small HOMO–LUMO gap implies that the Mo<sub>3</sub>S<sub>9</sub> clusters can act as both Lewis acids and Lewis bases, which is essential for catalytic reactions in HDS and probably Fischer–Tropsch synthesis.

**Acknowledgment.** Part of this work was supported by the Centre National de la Recherche Scientifique (Rennes, H.J.), and by the Alexander von Humboldt Stiftung (Erlangen, Y.-W.L.).

JA0034085